Unique Distribution of the Extracellular Matrix Component Thrombospondin in the Developing Mouse Embryo

K. S. O'Shea,* and V. M. Dixit‡

Departments of *Anatomy and Cell Biology and ‡Pathology, University of Michigan Medical School, Ann Arbor, Michigan 48109

Abstract. Immunocytochemical localization of thrombospondin (TSP), a trimeric glycoprotein constituent of extracellular matrices, produced striking regional and temporal patterns of distribution in the developing mouse embryo. TSP was present in many basement membranes, surrounded epithelial cells, and was associated with peripheral nerve outgrowth. During organogenesis, TSP was also found on the surface of myoblasts and chondroblasts, and TSP was differentially deposited in cortical layers. With differentiation of chondrocytes and myotubes immunoreactivity was decreased, and differential cortical staining was lost. Presence of TSP was associated with morphogenetic processes of proliferation, migration, and intercellular adhesion.

CELL migrations, cell–cell interactions, and, ultimately, cellular differentiation are directed in development by both genetic and epigenetic phenomena. Of the latter, the extracellular matrix (ECM)[1] (which is composed of tissue-specific proportions of collagens, proteoglycans, glycosaminoglycans, glycoproteins, water, and ions) appears to be of critical importance. In the current investigation, we have examined the deposition of a unique ECM component, thrombospondin (TSP), during the development of the mouse embryo.

TSP is a large glycoprotein (M_r 420,000) composed of three identical subunits in disulfide linkage (Dixit et al., 1984; Lawler et al., 1985). TSP was originally described as a platelet alpha granule component (Baenzinger et al., 1971) which was released on activation and became associated with the platelet surface to mediate platelet aggregation (Dixit et al., 1985). TSP is synthesized by a number of additional cells including smooth muscle (Raugi et al., 1982), endothelial cells (Mosher et al., 1982), keratinocytes (Wikner et al., 1987), macrophages (Jaffe et al., 1985), glia (Asch et al., 1986), and fibroblasts (Raugi et al., 1982). Like other large, adhesive glycoproteins, TSP may serve as an attachment factor for a variety of cells (Varani et al., 1986; Roberts et al., 1987). It appears to control proliferation and migration of smooth muscle cells (Majack et al., 1986) as well as chemotaxis of melanoma cells (Taraboldi et al., 1987).

TSP's widespread synthesis, its role in adhesion and in control of proliferation, as well as its rapid incorporation into and removal from the ECM, suggest that TSP may play an important role in regulating the structure of the extracellular milieu, and, thus, influence development. The current report describes striking alterations in the distribution of TSP during the development of the mouse embryo.

1. *Abbreviations used in this paper*: CNS, central nervous system; ECM, extracellular matrix; TSP, thrombospondin.

Materials and Methods

Tissue

Embryos were isolated from matings of CD-1 strain mice on days 9–17 of gestation (first day = + vaginal plug; gestation period = 19 d). Selected additional tissues from neonatal (postnatal day 10) or from adult mice were also examined. Because of the inherent difficulties in working with fresh frozen sections and for EM studies, numerous fixation protocols have been carried out in an attempt to improve tissue preservation and retain immunoreactivity. These protocols include fixation in: 10% formalin; 2 or 4% paraformaldehyde with and without 0.1–0.2% glutaraldehyde; phosphate, Tris, or cacodylate buffer; or by using the AMeX method (acetone fix at −20°C overnight; see Sato et al., 1986). Fixation periods varied from 30–120 min, and were followed by sodium borohydride (0.1%) treatment of whole embryos (or sections), and embedment in either OCT, paraffin, polyester wax (Kusakabe et al., 1984), or polyethylene glycol (water soluble). Because there was decreased anti-TSP immunoreactivity with any chemical fixative, the light microscopical results are based on sections of unfixed, frozen tissue.

Whole unfixed embryos and adult tissue were rapidly frozen in OCT embedding compound (Miles Laboratories Inc., Elkhart, IN) in hexane cooled over an acetone–dry ice slurry. Blocks were stored at −70°C before sectioning. Sagittal and transverse sections were cut at 8 μm and collected on 0.1% poly-L-lysine (molecular weight greater than 300,000) coated slides. At least 10 embryos at each developmental stage from a total of 128 were examined in the course of this study.

Immunocytochemistry

Selected sections were washed in PBS, and tissue was exposed to normal goat serum (1:20), followed by the primary antibody (TSP 1:20; type IV collagen 1:100) for 2 h at room temperature. Controls were exposed to PBS or to rabbit serum in place of the primary antibody. For preabsorption controls, sections were treated with a 1:20 dilution of antiserum that had been incubated previously with excess TSP in a proportion equivalent to 10 μg of purified TSP per 1 μg of rabbit anti-TSP IgG. All sections were subjected to similar rinses and incubation periods.

Sections were washed in PBS, exposed to the secondary antibody, goat anti-rabbit IgG conjugated to FITC (1:50), for 30 min at room temperature, and then washed thoroughly in PBS. Slides were coverslipped with glycerol containing 0.1% phenylenediamine and sealed. Sections were photographed in a Dialux Orthoplan photomicroscope (E. Leitz, Inc., Rockleigh, NJ) using Kodak Recording 2475 or Tri-X Pan film.

Because of the many interactions between ECM components, a number of pretreatments were used to augment the intensity of anti-TSP staining or to "restore" antigenicity to fixed tissue. Pretreatment of sections with testicular hyaluronidase (400 IU/ml for 1 h at 37°C)—but not with Streptomyces hyaluronidase (100 TRU/ml) nor collagenase (275 IU/ml, pH 7.4)—before exposure to the primary antibody, resulted in the altered patterns of staining for TSP described below, but no treatment augmented staining intensity.

For electron microscopic localization of TSP, tissue was briefly fixed in 2% paraformaldehyde and 0.1% glutaraldehyde in 0.1 M phosphate buffer for 45 min at room temperature. It was then vibratome sectioned in agar (13%) at 50 μm, and slices were washed and stored in 0.1 M phosphate buffer before staining. Slices were preincubated in 5% normal goat serum in PBS also containing 2% BSA for 2 h at room temperature and rinsed in PBS with 1% BSA. Slices were next exposed to the primary antibody made up in PBS with 1% BSA for 15 min at room temperature and then at 4°C overnight. Tissue was rinsed; fixed in 1.5% glutaraldehyde in 0.1 M cacodylate buffer (pH 7.4) with 5% sucrose for 1 h at room temperature; and then rinsed in 0.1 M cacodylate buffer followed by an additional rinse in 50 mM Tris-HCl buffer (pH 7.4). Slices were then incubated in 0.1% diaminobenzadine with 0.01% hydrogen peroxide in 50 mM Tris-HCl buffer for 10 min. After an additional rinse, slices were stained in 1% osmium tetroxide and 1% potassium ferrocyanide in 0.1 M cacodylate buffer for 45 min at 4°C. Slices were rinsed, dehydrated through graded alcohols, embedded in Araldite resin, sectioned, viewed, and photographed in an electron microscope (model 400; Philips Electronic Instruments, Inc., Mahwah, NJ). For EM localization, anti-TSP was used at 1:10 and antibodies to the glial fibrillary acidic protein were used at 1:50. Additional controls were exposed either to normal rabbit serum diluted 1:50 or to PBS alone.

Antibodies

Rabbit polyclonal antibody to TSP was obtained and characterized as described previously (Roberts et al., 1985; Varani et al., 1986). Briefly, rabbit antisera was raised to human platelet TSP and the IgG fraction purified on a protein A–Sepharose column (Bio-Rad Laboratories, Richmond, CA). The antibody, as assayed by radioimmunoassay (Dixit et al., 1985) and immunoprecipitation of metabolically labeled human carcinoma cells (Varni et al., 1986), was specific for TSP. Antibody to type IV collagen was purchased from Dr. H. Furthmayr (Yale University), was affinity purified and exhibited no cross-reactivity to other ECM components when examined using ELISA. Antibody to the glial fibrillary acidic protein was purchased from Dakopatts (Copenhagen).

Cell Culture

Mouse NIH 3T3 cells were maintained in DME supplemented with 10% FCS, penicillin (100 U/ml), and streptomycin (100 μg/ml). All culture materials were purchased from Gibco Laboratories (Grand Island, NY).

Biosynthetic Labeling and Immunoprecipitation

Mouse NIH 3T3 cells were grown in 100-mm culture dishes to an approximate density of 2×10^6 cells/dish. The cells were washed twice in serum-free DME without cysteine and methionine and were incubated overnight in the same medium supplemented with 10% dialyzed FCS, 100 μCi/ml of [^{35}S]methionine (1,000–1,400 μCi/μM; New England Nuclear, Boston, MA) and 100 μCi/ml of [^{35}S]cysteine (937 Ci/mmol; New England Nuclear). Metabolic labeling with both [^{35}S]methionine and [^{35}S]cysteine was done in order to minimize any bias in labeling of proteins that may be deficient in one or the other amino acid.

The medium was removed and the cells lysed in a solution of PBS that contained detergents (1% Triton X-100, 0.5% sodium deoxycholate, and 0.1% SDS; Sigma Chemical Co., St. Louis, MO) and protease inhibitors including 20 mM EDTA, 5 mM *N*-ethylmaleimide, and 2 mM PMSF. The labeled medium was also supplemented with the detergent/protease inhibitor mixture by adding 0.25 vol of a fivefold concentrated solution. The labeled cell lysates and media were mixed and clarified by ultracentrifugation (37,000 *g* for 60 min).

Immunoreactive TSP was precipitated with a 1:100 dilution of the rabbit anti-TSP and protein A–Sepharose (Pharmacia, Uppsala, Sweden) as described previously (Dixit et al., 1985). Affinity-purified rabbit anti-mouse IgG served as a control. Washed immunoprecipitates were eluted by boiling (5 min) in Laemmli SDS-PAGE sample buffer with 2% 2-mercaptoethanol and resolved on a 4–12% gradient Laemmli polyacrylamide gel (Dixit et al., 1985). Radiolabeled proteins were visualized by fluorography with EN^{3}HANCE (New England Nuclear).

Tissue Immunoblotting

Day-13 embryos were homogenized with a Polytron tissue homogenizer in Laemmli SDS-PAGE sample buffer. Soluble proteins were resolved on a 7.5% Laemmli polyacrylamide gel and electrophoretically transferred to nitrocellulose paper. Nonspecific binding was blocked by incubating the blots with 3% BSA for 2 h at room temperature.

The blots were next incubated with either rabbit anti-TSP (1:100) or control antibody (rabbit anti-mouse IgG) in 0.02 M Tris HCl, pH 7.5; 0.5 M NaCl; 1% BSA for 1 h at room temperature. Transfers were rinsed twice with the above buffer containing 0.05% Tween 20 and then incubated with horseradish peroxidase–conjugated goat anti-mouse IgG for 2 h at room temperature. After several washes with the Tween-containing buffer, peroxidase activity was detected with 4-chloronaphthol and hydrogen peroxide.

Results

Antibody Specificity

The rabbit anti-TSP antibody used in these studies has been previously shown to be specific for human TSP because it will specifically and quantitatively immunoprecipitate TSP from [^{35}S]methionine-labeled human squamous carcinoma cells (Varani et al., 1986). To ensure specificity of the antibody for mouse TSP, we metabolically labeled mouse NIH 3T3 cells with [^{35}S]methionine and [^{35}S]cysteine and subjected total labeled proteins (both media and cell lysate) to immunoprecipitation.

As illustrated in Fig. 1, the rabbit anti-TSP antibody (lane *3*), unlike a control antibody (lane *4*), specifically immunoprecipitated a protein that comigrates with an iodinated TSP marker (lane *1*). Even after prolonged exposure of the autoradiogram, TSP was the only protein immunoprecipitated by the rabbit anti-TSP antibody.

To further ensure the specificity of the antibody used in these studies, a tissue immunoblotting was carried out (Fig. 2). Soluble protein extract from day-13 mouse embryos was resolved by SDS-PAGE, transferred to nitrocellulose, and reacted with rabbit anti-TSP or control antibody. As shown in Fig. 2, rabbit anti-TSP detected a protein in embryonic tissue extracts (lane *4*) that comigrated with purified human platelet TSP (lane *6*). Control antibody showed no reactivity to either (lanes *7* and *9*).

Immunocytochemistry

Immunocytochemical results are presented according to developmental stage: (*a*) neurulation (days 9–11); (*b*) organogenesis (days 13, 15); and (*c*) fetal period (day 17). No immunoreactivity was observed in tissues exposed to PBS in place of the primary antibody nor with preabsorption controls. When normal rabbit serum replaced the primary antibody, there was slight staining only of the forming perichondrium (Fig. 3 *f*). This pattern was observed on each day of development examined. The contribution of platelet TSP to

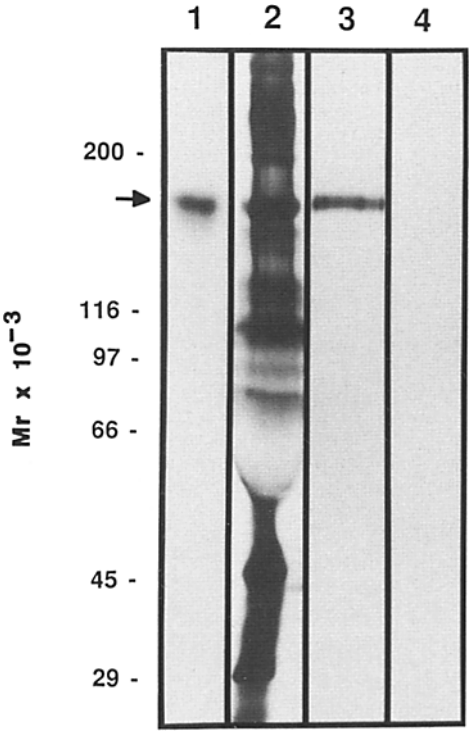

Figure 1. Specificity of rabbit anti-TSP antibody. Mouse NIH 3T3 cells were metabolically labeled with [^{35}S]cysteine and [^{35}S]methionine and total labeled proteins (lane *2*) were immunoprecipitated either with rabbit anti-TSP (lane *3*) or control antibody (lane *4*). Arrow indicates the position of migration of an iodinated human platelet TSP standard (lane *1*). Proteins were resolved by SDS-PAGE on a 4–12% gradient Laemmli gel and visualized by autoradiography. Kodak X-OMAT AR film was exposed overnight at −80°C.

staining was negligible because of the paucity of platelets in early embryos.

Neurulation (Days 9–11). During this period, mouse embryos develop from 5 to 38 somites, the embryo rotates to adopt the fetal position, and the heart tube forms (Fig. 3, *a* and *b*). During this period, TSP was present in basement membranes of the surface ectoderm and neuroepithelium (Fig. 4 *a*) and was densely deposited between neuroepithelial cells (Fig. 3, *a* and *b*; Fig. 4, *a* and *b*). TSP was particularly densely deposited in the neural crest migratory pathway at the dorsolateral surface of the neuroepithelium. With aggregation of neural crest to form ganglia, TSP was present on the surface of aggregating cells (Fig. 4 *a*). At the later phases of this stage, TSP outlined processes emerging from the ventral neuroepithelium (Fig. 4 *b*).

TSP was found in the epimyocardium and epicardium of the heart (Fig. 4, *c* and *d*) but was not yet a component of the endocardium or of forming blood vessels (Fig. 3, *a* and *b*). TSP was also found in forming somites, especially in the outer, epithelial portions (Fig. 4 *e*). In the liver by the 10th day of development, a regional population of cells was intensely stained (Fig. 4 *f*).

When sections were pretreated with testicular hyaluronidase, the pattern of immunoreactivity was altered. In the developing optic vesicle for example, TSP was present between neuroepithelial cells and in the neuroepithelial basement membrane (Fig. 4 *g*). After testicular hyaluronidase treatment, staining was present in the basement membrane, but not within the neuroepithelium itself (Fig. 4 *h*).

Organogenesis (Days 13, 15). During organogenesis, TSP was a less general component of the developing embryo, becoming associated more clearly with specific cell populations (Fig. 3, *c* and *d*).

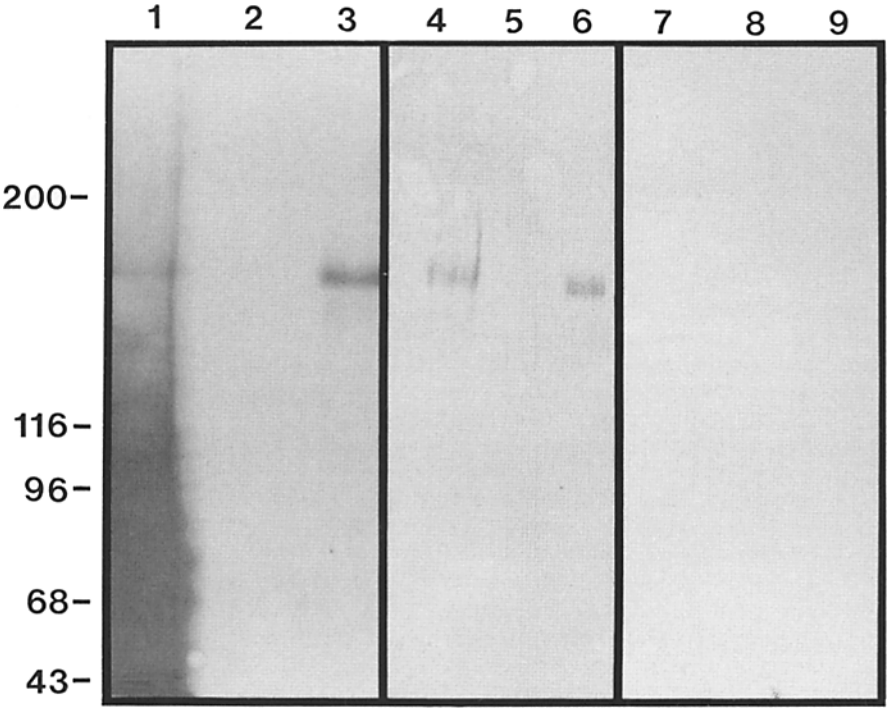

Figure 2. Specificity of rabbit anti-TSP shown by tissue immunoblotting. Solubilized 13-d mouse embryo extract (lanes *1*, *4*, and *7*) and purified human TSP (lanes *3*, *6*, and *9*) were resolved by SDS-PAGE and transferred to nitrocellulose paper. Lanes *2*, *5*, and *8* were left blank to ensure no "spill-over" of material between lanes. Lanes *1–3* were stained for protein (Amido black); lanes *4–6* were allowed to react with rabbit anti-TSP; lanes *7–9* were allowed to react with control antibody. Immune complexes were visualized by incubation with horseradish peroxidase–conjugated goat anti-mouse IgG. Molecular mass markers in kilodaltons are shown (*left*).

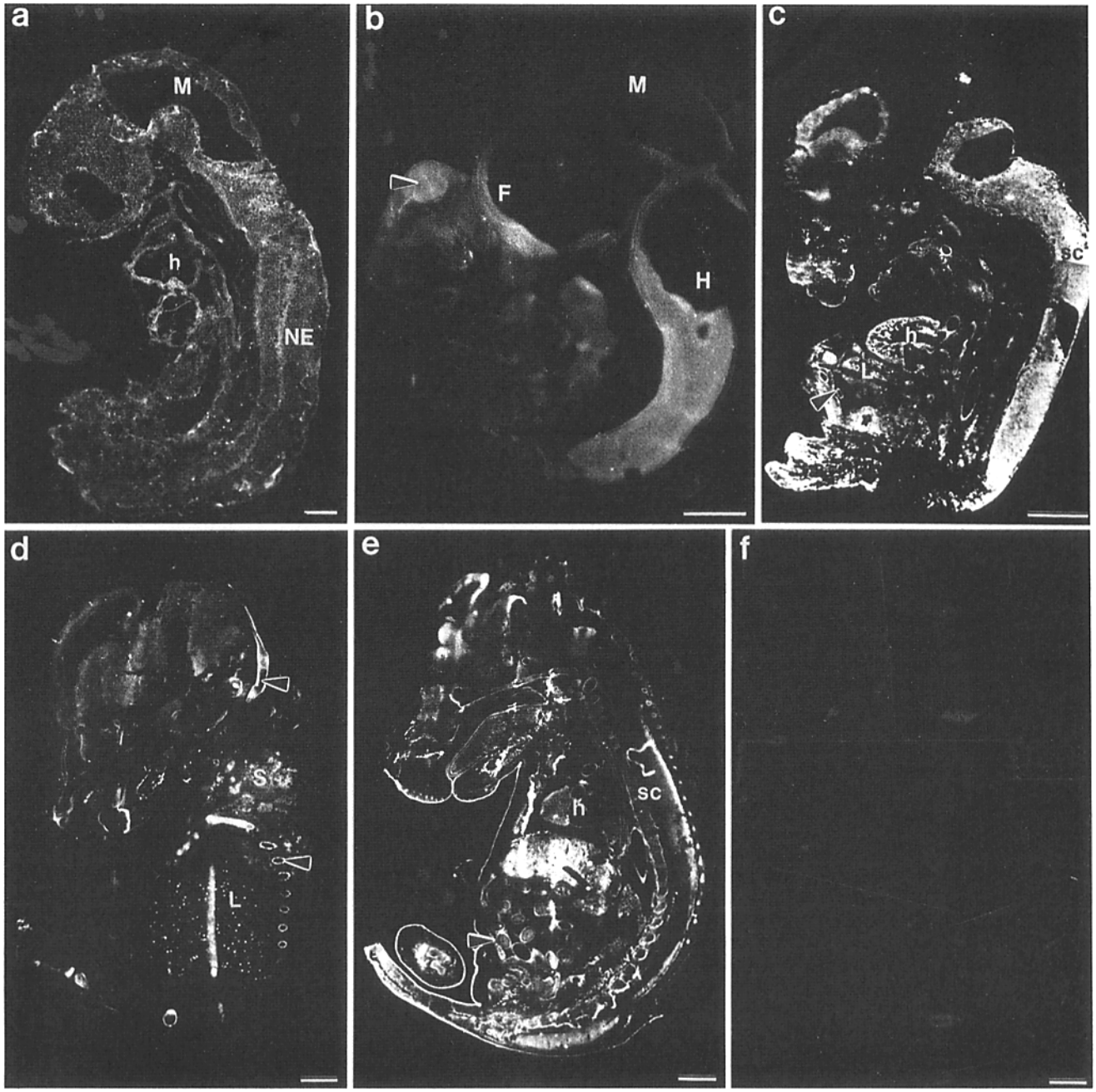

Figure 3. Sagittal sections through embryos isolated on days 10–17 of gestation illustrating the pattern of deposition of TSP (*a–e*), and lack of immunoreactivity in a control embryo (*f*). Embryos are oriented with their cephalic region toward the top of the micrographs and their dorsal surface toward the right. (*a*) Sagittal section through a day-10 embryo. TSP was densely deposited in the forming CNS and heart. *M*, midbrain; *h*, heart; *NE*, neuroepithelium. Bar, 100 μm. (*b*) Day-11 embryo illustrating the dense deposition of TSP in the forebrain (*F*), hindbrain (*H*), and spinal cord (*arrow*) at this stage of development. *M*, midbrain. Bar, 500 μm. (*c*) Day-13 embryo illustrating pattern of deposition of TSP in the CNS and developing heart (*h*), in forming liver (*L*), and in gut (*arrow*), *sc*, forming spinal cord. Bar, 1 mm. (*d*) On day 15 TSP was present in the CNS, in forming cartilage (*arrows*), and in skeletal muscle (*S*). Scattered hepatic cells stained strongly for TSP as did salivary gland, forming bronchi in the lung and herniated gut. The vertical "line" coursing through the liver (*L*) is a fold in the tissue. Bar, 1 mm. (*e*) Sagittal section through a day-17 embryo. TSP was present in many basement membranes, in the heart (*h*), skin, perichondrium, and gut (*arrow*). Although present, it was a less prominent component of the CNS and of chondrocytes than at previous stages, *sc*, spinal cord. Bar, 1 mm. (*f*) Day-15 control embryo incubated in normal rabbit serum rather than anti-TSP IgG illustrating the general lack of immunofluorescence. Light perichondrial stain was observed with normal rabbit serum that was not present in preabsorption or in PBS controls. Similar results were obtained at each developmental stage examined. Bar, 1 mm.

Figure 4. Survey of TSP localization in several organs at the earliest stages of development examined (days 9–11). (*a*) Transverse section through the region of crest cell migration from the neuroepithelium (*NE*) late on day 9 of development. Note the dense deposition of TSP between neuroepithelial cells, in the migration zone and in the neuroepithelial basement membrane (*arrow*). Bar, 100 μm. (*b*) Transverse section through the neuroepithelium in a day-10 embryo, illustrating the deposition of TSP between neuroepithelial cells (*NE*). It was also particularly densely deposited in the ventral root pathway (*arrow*). Bar, 100 μm. (*c*) Sagittal section through the developing heart tube illustrating the dense deposition of TSP in the epimyocardium and epicardium, but little staining in the forming endocardium on the 10th day. Bar, 100 μm. (*d*) Higher magnification of the wall of the heart tube illustrating TSP deposition in the epimyocardium (*e*) and forming epicardium (*ep*). Bar, 50 μm. (*e*) Sagittal section through two adjacent somites (*S*) from the spinal region late on day 9 of development. TSP was particularly densely deposited between cells in the outer epithelial layer (*arrow*), compared to the core of the somites (sclerotome).

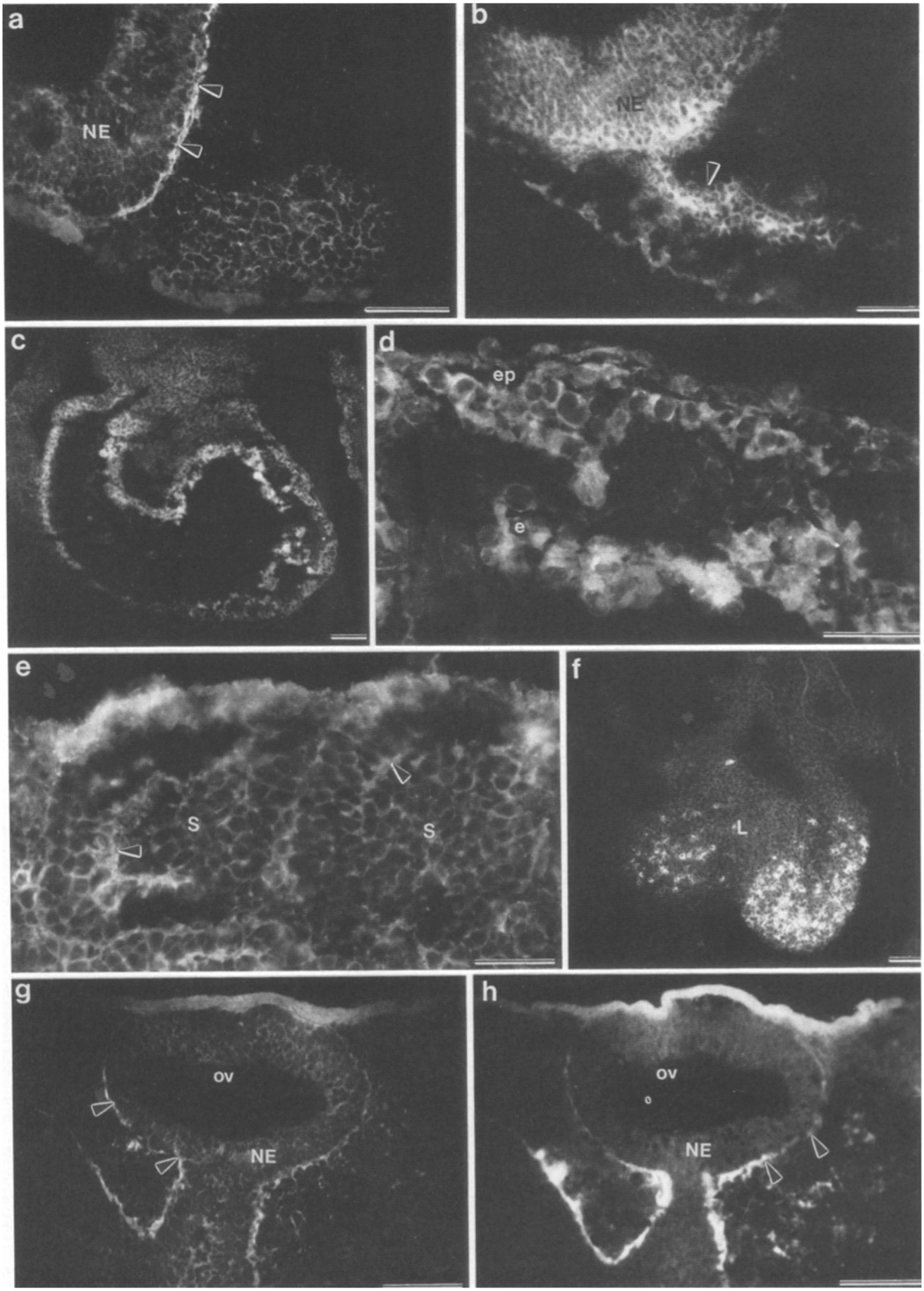

Bar, 50 μm. (*f*) Unlike later stages of development, a large proportion of cells in the liver (*L*) stained intensely for TSP on day 11 of gestation. Bar, 100 μm. (*g*) On day 10, TSP was densely deposited in the neuroepithelium (*NE*) and basement membrane (*arrow*) of the optic vesicle (*ov*). Bar, 100 μm. (*h*) Sequential section through the optic vesicle (*ov*) pretreated with testicular hyaluronidase before localization of TSP. TSP was present in the basement membrane (*arrow*) but was no longer demonstrable between neuroepithelial cells (*NE*). Bar, 100 μm.

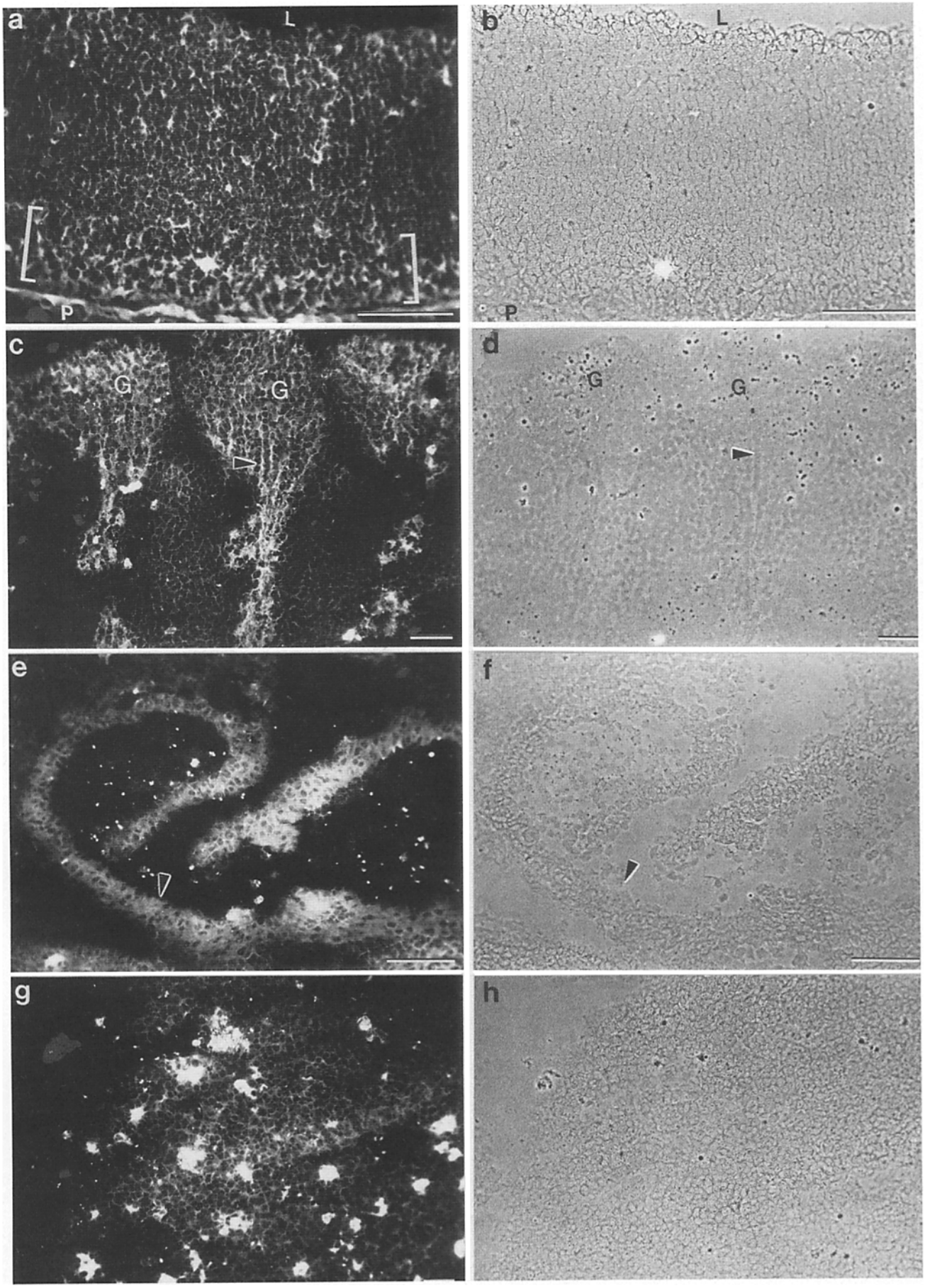
a
L
P
b
L
P
c
G
G
d
G
G
e
f
g
h

On the 13th day, TSP continued to surround neuroepithelial cells and was present in the neuroepithelial basement membrane at the pial surface (Fig. 5, *a* and *b*). In the cortex, TSP was differentially deposited in the developing cortical layers. The cortical plate and forming glial endfeet regions stained particularly densely (Fig. 5, *a* and *b*). Ganglia (cephalic, dorsal root, and autonomic) also contained dense deposits of TSP (Fig. 5, *c* and *d*), and nerve rootlets emerging from dorsal root ganglia were intensely stained. TSP was present in the epicardium and forming myoepicardium as well as in the endocardium of the heart (Fig. 5, *e* and *f*). TSP was present in a subset of liver cells (Fig. 5, *g* and *h*) and outlined the basement membrane of the forming bronchi in the lung.

By day 15, the population of presumably hematopoietic cells present in the liver continued to stain and now were diffusely distributed rather than forming clusters (Fig. 3 *d*). In the central nervous system (CNS), TSP surrounded neuroepithelial cells (Fig. 6, *a* and *b*) and was deposited at the pial surface and near the lumen. In the cerebellar anlagen near the fourth ventricle, radial deposits of TSP extended from the rhombic lip across the developing cerebellum. In the lung, salivary gland, and kidney, TSP was found between cells and particularly in basement membranes (Fig. 6, *c* and *d*). On day 15, undifferentiated myoblasts contained considerable TSP on their surfaces (Fig. 6, *e* and *f*) as did chondroblasts (Fig. 6, *g* and *h*). As chondrocytes hypertrophied, beginning on the 15th day, the deposition of TSP on their surfaces was reduced (Fig. 6, *g* and *h*).

Early Fetal Development (Day 17). During later phases of development, the pattern of TSP deposition remained somewhat similar to that seen on days 13 and 15 with important exceptions (Fig. 3 *e*). In the nervous system, although less prominently than at earlier stages, TSP continued to surround neuroepithelial cells but without the obvious layering observed earlier (Fig. 7, *a* and *b*). By day 17, the radial deposits observed in the cerebellar cortex on day 15 were no longer present, but TSP was densely deposited just below the pial surface. Growing peripheral nerve continued to stain strongly for TSP.

By the 17th day, there was a reduction in the proportion of hepatic cells that were stained. TSP remained present in epithelia and their basement membranes in lung (Fig. 7, *c* and *d*), salivary gland, and colonic epithelium. By the 17th day, endothelial cells lining larger vessels (Fig. 7, *c* and *d*) were stained as was the choroid plexus of the fourth ventricle. As myoblasts that had contained considerable TSP on their surfaces fused to form multinucleate myotubes, TSP was much less prominent on their surfaces (Fig. 7, *e* and *f*). In the skin, TSP was distributed between cells and was present in the basement membrane at the forming dermal epidermal junction (Fig. 7, *g* and *h*) and at developing hair follicles and vibrissae.

In an attempt to further characterize the presence of TSP in basement membranes, we examined a number of additional tissues from older animals including lung, ovary, placenta, nerve, brain, and liver. When examined at the light level, TSP was present in basement membranes of epithelial cells from these organs, and often TSP was found in association with lateral cell surfaces as well. For example, the basement membrane separating granulosa and theca interna cells in developing ovarian follicles contained considerable TSP with slight cell surface stain (Fig. 8 *a*). By comparison, type IV collagen was more clearly restricted to the basement membrane (Fig. 8 *b*).

At the electron microscopic level, TSP was clearly deposited in basal laminae (see Fig. 8 *c*, for example in a capillary endothelial cell). Neither localization of an "irrelevant antibody," normal rabbit serum, nor replacement of the primary antibody with PBS revealed any basal lamina reactivity. Localization of antibodies to the glial fibrillary acidic protein resulted in restriction of reaction product to astrocytic cytoplasm in the cerebellar cortex (Fig. 8 *d*).

Discussion

This is the first report of the striking regional and temporal patterns of TSP deposition during development. Although a comprehensive discussion of the role of TSP in the morphogenesis of the individual tissues is clearly beyond the scope of the current investigation, several broad patterns emerge.

At the earliest stages examined, TSP was densely deposited between neuroepithelial cells as the neural folds elevated, met, and fused in the dorsal midline of the embryo. TSP was present in basement membranes and was less densely deposited in the mesenchyme although TSP surrounded neural crest cells as they migrated and also as they aggregated to form ganglia. This pattern has not previously been reported during early development since laminin, fibronectin, type IV collagen, heparan sulfate proteoglycan (Tuckett and Morriss-Kay, 1986; Sternberg and Kimber, 1986; O'Shea, 1987) are present in neuroepithelial basement membranes; fibronectin and heparan sulfate proteoglycan (Sternberg and Kimber, 1986; O'Shea, 1987) are additional mesenchymal components. Presence of TSP on neuroepithelial cells at this stage parallels only the deposition of the neural cell adhesion molecule (Thiery et al., 1982) and of the fibronectin receptor (Duband et al., 1986)—but not of fibronectin itself—in avian embryos. Localization of the cell substratum attachment (CSAT) receptor complex is similar to TSP in that it surrounds neuroepithelial cells, neural crest, and dorsal root ganglia, and is found in basement membranes as well (Krotoski et al., 1986).

In the peripheral nervous system at all stages examined, TSP was associated with outgrowing nerve processes. Laminin has a distribution similar to TSP during early outgrowth

Figure 5. Sagittal sections of several tissues from day-13 embryos. *a*, *c*, *e*, and *g* illustrate depositional patterns of TSP. *b*, *d*, *f*, and *h* represent the corresponding phase-contrast micrographs. (*a* and *b*) Cerebral cortex and pial surface (*p*) illustrating the deposition of TSP on neuroepithelial cell surfaces and in the forming pia mater. TSP was also particularly densely deposited at this stage in the cortical plate region (*brackets*). *L*, lumen of the neural tube. (*c* and *d*) Grazing sagittal section illustrating nerve roots (*arrow*) and associated dorsal root ganglia (*G*). (*e* and *f*) Section through a portion of the heart tube illustrating TSP deposition in the forming myocardium and in the endocardium (*arrow*) at this stage of development. (*g* and *h*) A subset of hepatic cells continued to stain intensely for TSP. Bars, 100 μm.

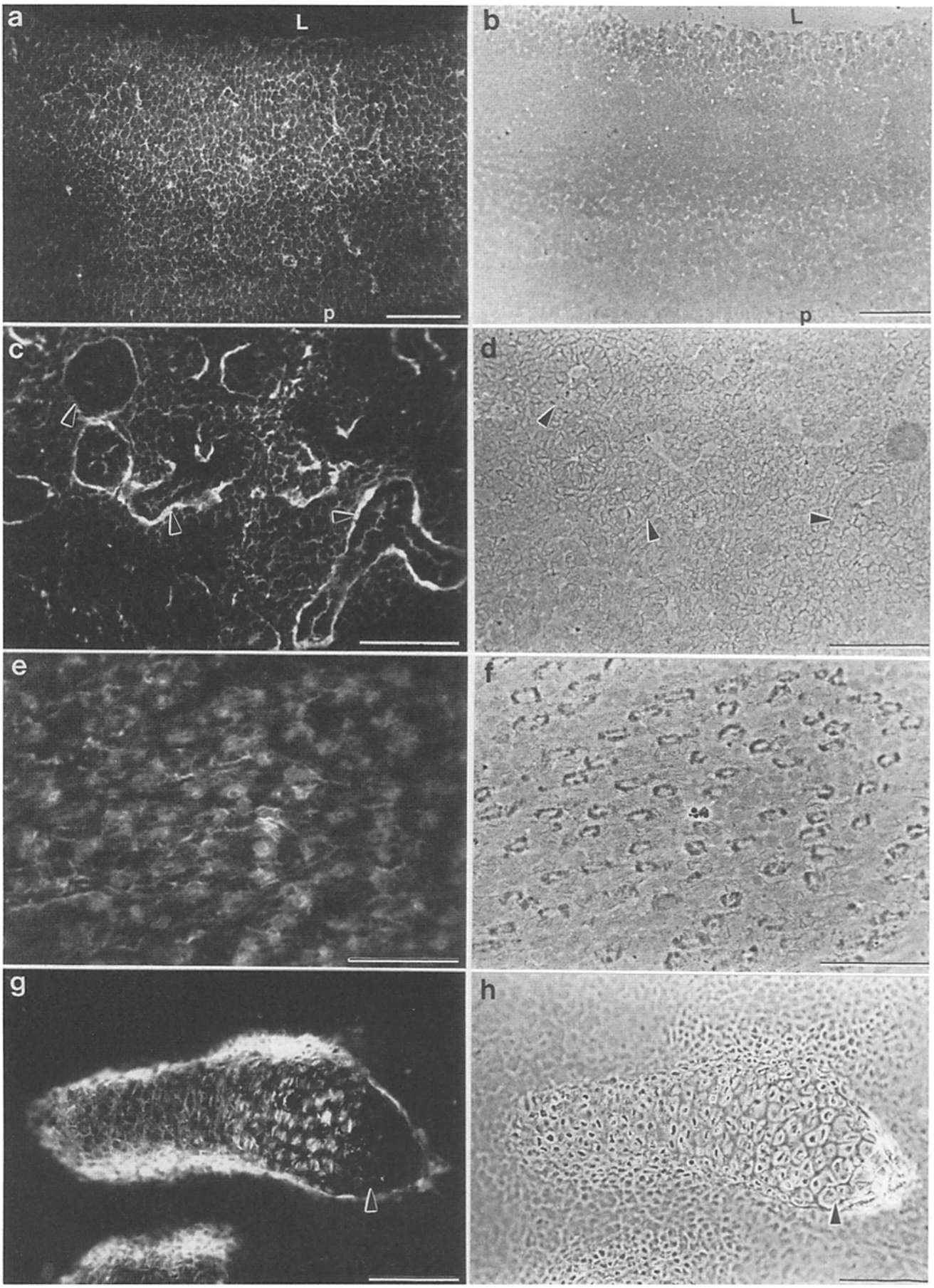
a
L
p
b
L
p
c
d
e
f
g
h

from the neuroepithelium (Rogers et al., 1986), and HNK-1/NC-1 is similarly found in the ventral horn in the region of motor neuron axon outgrowth (Tucker et al., 1988). In later consolidation of the nerve, however, the patterns are considerably different. The presence of TSP on both migrating and aggregating neural crest cells is also unparalleled by other ECM components. Fibronectin, for example, is present during neural crest cell migration but is largely displaced from between crest cells as they aggregate to form ganglion rudiments (Duband et al., 1985).

Presence of TSP in regions of cell migration and rearrangement may be associated with its ability to bind both plasminogen and tissue plasminogen activator. This binding greatly enhances plasminogen activation by tissue plasminogen activator (Silverstein et al., 1984, 1985, 1986). It is possible that TSP may form a nidus for protease generation during cellular migrations and tissue remodeling critical in early development. Although the distribution of tissue plasminogen activator during early embryogenesis has not been precisely determined, tissue plasminogen activator is similarly present during granule cell migration in the cerebellum (Krystosek and Seeds, 1981), during neurite outgrowth (Patterson, 1985), and in the development of the peripheral nervous system (Baron-VanEvercooren et al., 1987).

TSP was densely deposited in many basement membranes including neuroepithelial; surface ectodermal (later in the dermal epidermal junction, see also Wight et al., 1985); of salivary gland; gut; kidney; and lung; in ovarian follicles. In certain of these regions, TSP was deposited in association with regions of branching like other ECM components (e.g., Bernfield et al., 1984). However, unlike other matrix components TSP was also present between epithelial cells as the basement membrane formed. Testicular hyaluronidase sensitivity of cell surface, but not basement membrane, TSP suggests that TSP present in the basement membrane may associate not only with glycosaminoglycans but also with other ECM components, which decrease its susceptibility to being released by hyaluronidase treatment.

TSP is capable of binding a number of ligands: glycosaminoglycans (Dixit et al., 1984; Lawler et al., 1985), fibronectin (Lahav et al., 1982, 1984), plasminogen (Silverstein et al., 1984), laminin (Mumby et al., 1984), types I and V collagen (Lahav et al., 1982; Mumby et al., 1984). Because of the affinity of TSP for many ECM components and its rapid removal from and incorporation into the ECM via its heparan binding domain (McKeown-Longo et al., 1984), TSP may play an important role in determining the structural characteristics of the matrix associated with these tissues.

Somewhat surprisingly, there was little TSP present in early forming blood vessels, unlike laminin and type IV collagen which are present very early in the forming basement membrane of these vessels (O'Shea, 1987). At later stages of development, TSP was clearly present in endothelial cells as well as in the endocardium. It will be interesting to determine whether or not TSP becomes associated with smooth muscle cells of the vessel wall with the significant pressure alterations at birth.

Interestingly, TSP immunoreactivity present on the surface both of chondroblasts (see also Miller and McDevitt, 1988) and myoblasts was decreased with differentiation. Whether the presence of TSP (*a*) is associated with cellular proliferation, as in other systems (Majack et al., 1986), or (*b*) plays a role in controlling cell-cell interactions remains to be determined. It will be interesting to examine the detailed pattern of deposition within the sclerotome during earlier development and to determine the pattern of deposition in mature skeletal muscle.

Not surprisingly, TSP is associated with several very different morphogenetic processes, including cellular migrations, proliferation, and intercellular adhesion possibly by controlling the structure of the matrix itself and thus influencing gene expression. Current investigations are in progress to examine additional periods of development and to determine the pattern of synthesis of this important ECM component.

The authors are grateful to Jill and Terry Rheinheimer for excellent photographic assistance and to Karen O'Rourke and L-H. J. Liu for technical assistance.

This work was supported by grants NS-21108, HL-39415, and HD-23867 from the National Institutes of Health.

Received for publication 8 February 1988, and in revised form 2 September 1988.

References

Asch, A. S., L. L. K. Leung, J. Shapiro, and R. L. Nachman. 1986. Human brain glial cells synthesize thrombospondin. *Proc. Natl. Acad. Sci. USA.* 83: 2904–2908.

Baenzinger, N. L., G. N. Brodie, and P. W. Majerus. 1971. A thrombin-sensitive protein of human platelet membranes. *Proc. Natl. Acad. Sci. USA.* 68:240–243.

Baron-VanEvercooren, A., P. Leprince, B. Rogister, P. P. Lefebvre, P. Delree, I. Selak, and G. Moonen. 1987. Plasminogen activators in developing peripheral nervous system, cellular origin and mitogenic effect. *Dev. Brain Res.* 36:101–108.

Bernfield, M., S. D. Banerjee, J. E. Koda, and A. C. Rapraeger. 1984. Remodeling of the basement membrane: morphogenesis and maturation. *CIBA Found. Symp.* 108:179–191.

Dixit, V. M., G. A. Grant, S. A. Santoro, and W. A. Frazier. 1984. Isolation and characterization of a heparin-binding domain from the amino terminus of platelet thrombospondin. *J. Biol. Chem.* 259:10100–10105.

Dixit, V. M., D. M. Haverstick, K. M. O'Rourke, S. W. Hennessy, G. A. Grant, S. A. Santoro, and W. A. Frazier. 1985. A monoclonal antibody against human thrombospondin inhibits platelet aggregation. *Proc. Natl. Acad. Sci. USA.* 82:3472–3476.

Duband, J.-L., G. C. Tucker, T. J. Poole, M. Vincent, H. Aoyama, and J. P. Thiery. 1985. How do the migratory and adhesive properties of the neural crest govern ganglia formation in the avian peripheral nervous system? *J. Cell. Biochem.* 17:189–203.

Duband, J.-L., S. Rocher, W.-T. Chen, K. M. Yamada, and J. P. Thiery. 1986. Cell adhesion and migration in the early vertebrate embryo: location and pos-

Figure 6. Sagittal sections through several organs from day-15 embryos illustrating the deposition of TSP (*a*, *c*, *e*, and *g*) and corresponding phase-contrast micrographs (*b*, *d*, *f*, and *h*). (*a* and *b*) Differential deposition of TSP associated with the forming cortical layers. Note the change in the pattern of deposition compared to that seen on day 13, particularly in the cortical plate region. *L*, lumen of the neural tube, *p*, pial surface. (*c* and *d*) TSP was associated with basement membranes (*arrow*) of the forming bronchial tree. (*e* and *f*) Myoblast cell surfaces in the lower limb were intensely stained. (*g* and *h*) Forming cartilage illustrating the dense deposition of TSP on chondroblasts and in the forming perichondrium. TSP deposition was greatly reduced in regions of hypertrophy (*arrow*). Bars, 100 μm.

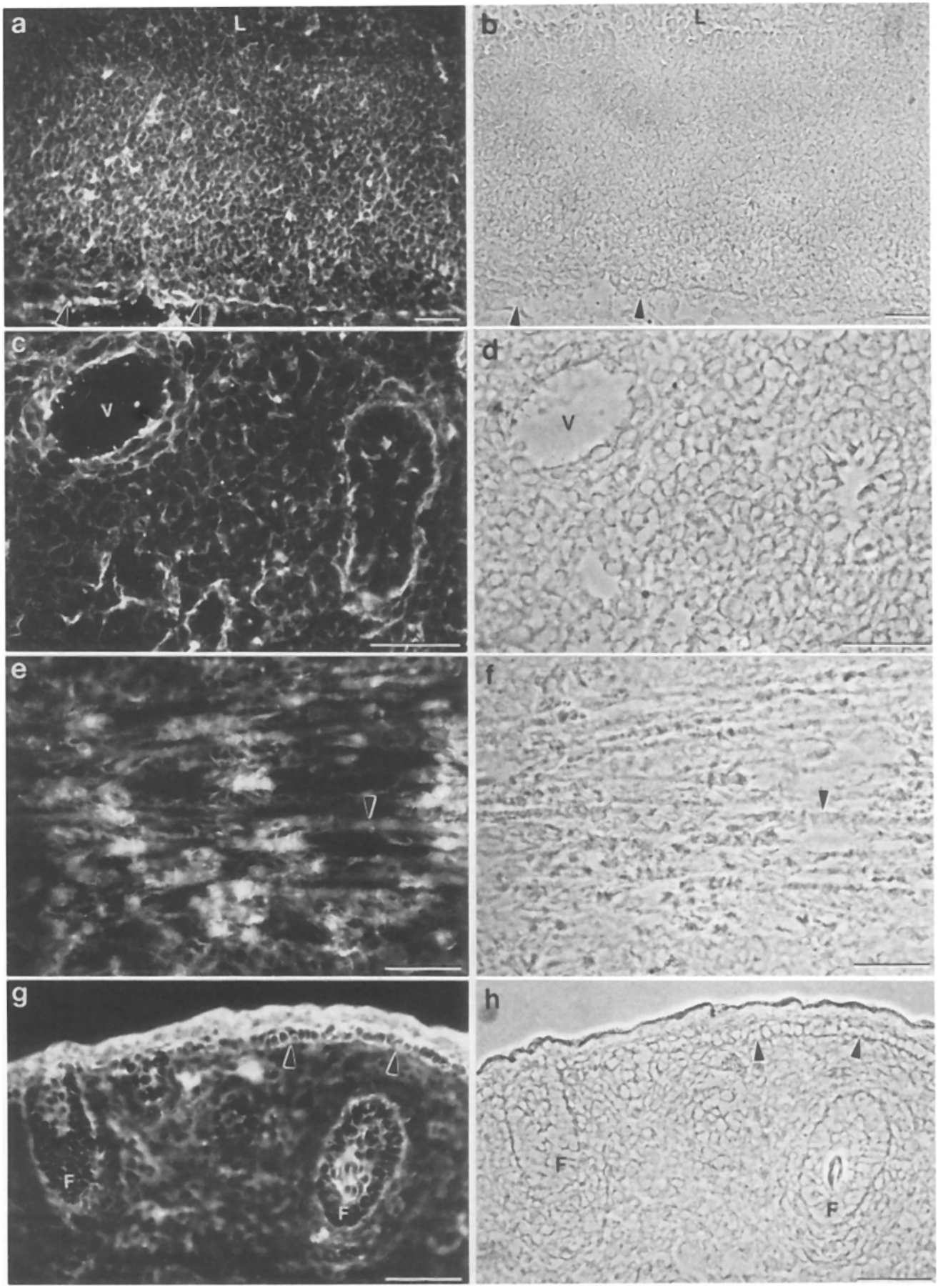
a
L
b
L
c
V
d
V
e
f
g
F
F
h
F
F

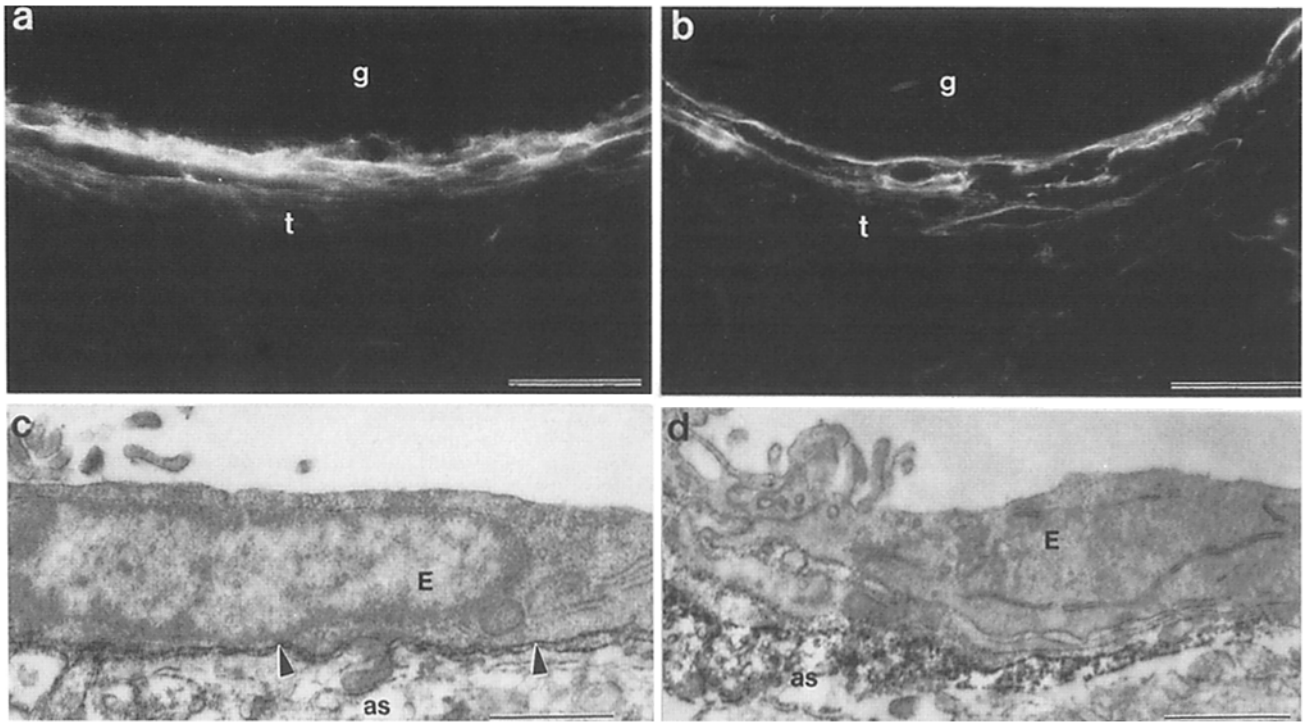

Figure 8. Micrographs illustrating the deposition of thrombospondin (*a* and *c*) or type IV collagen (*b*) in basement membranes. *d* illustrates EM localization of an "irrelevant antibody," the glial fibrillary acidic protein. (*a*) TSP was densely deposited in the basement membrane that separates granulosa cells (*g*) and theca interna (*t*) in a vesicular ovarian follicle. Bar, 25 μm. (*b*) Sequential section through the same follicle stained with anti-type IV collagen illustrating the similar localization in the basement membrane between granulosa (*g*) and thecal cells (*t*), and in the basement membrane of thecal vessels. Bar, 25 μm. (*c*) Electron microscopic localization of TSP in the basal lamina (*arrow*) of a capillary endothelial cell (*E*) in the cerebellar cortex on postnatal day 10. An astrocytic endfoot (*as*) surrounds the capillary endothelial cell. Bar, 1 μm. (*d*) Similar capillary endothelial cell from a day-10 postnatal cerebellum stained with antibodies to the glial fibrillary acidic protein, illustrating the lack of staining in the capillary endothelial (*E*) basal lamina, but dense reaction product in the astrocytic (*as*) cytoplasm. Bar, 1 μm.

sible role of the putative fibronectin receptor complex. *J. Cell Biol.* 102:160–178.

Jaffe, E. A., J. T. Ruggiero, and D. J. Falcone. 1985. Monocytes and macrophages synthesize and secrete thrombospondin. *Blood.* 65:79–84.

Krotoski, D. M., C. Domingo, and M. Bronner-Fraser. 1986. Distribution of a putative cell surface receptor for fibronectin and laminin in the avian embryo. *J. Cell Biol.* 103:1061–1071.

Krystosek, A., and N. W. Seeds. 1981. Plasminogen activator secretion by granule neurons in cultures of developing cerebellum. *Proc. Natl. Acad. Sci. USA.* 78:7810–7814.

Kusakabe, M., T. Sakakura, Y. Nishizuka, M. Sano, and A. Matasukage. 1984. Polyester wax embedding and sectioning technique for immunohistochemistry. *Stain Technol.* 59:127–132.

Lahav, J., M. A. Schwartz, and R. O. Hynes. 1982. Analysis of platelet adhesion with a radioactive chemical crosslinking reagent. Interaction of thrombospondin with fibronectin and collagen. *Cell.* 31:253–262.

Lahav, J., J. Lawler, and M. A. Gimbrone. 1984. Thrombospondin interactions with fibronectin and fibrinogen: mutual inhibition in binding. *Eur. J. Biochem.* 145:151–156.

Lawler, J., L. H. Derick, J. E. Connolly, J.-H. Chen, and F. C. Chao. 1985. The structure of human platelet thrombospondin. *J. Biol. Chem.* 260:3762–3772.

Majack, R. A., S. C. Cook, and P. Bornstein. 1986. Control of smooth muscle cell growth by components of the extracellular matrix: autocrine role for thrombospondin. *Proc. Natl. Acad. Sci. USA.* 83:9050–9054.

McKeown-Longo, P. J., R. Hanning, and D. F. Mosher. 1984. Binding and degradation of platelet thrombospondin by cultured fibroblasts. *J. Cell Biol.* 98:22–28.

Miller, R. R., and C. H. McDevitt. 1988. Thrombospondin is present in articular cartilage and is synthesized by articular chondrocytes. *Biochem. Biophys. Res. Commun.* 153:708–714.

Mosher, D. F., M. J. Doyle, and E. A. Jaffe. 1982. Synthesis and secretion of thrombospondin by cultured human endothelial cells. *J. Cell Biol.* 93:343–348.

Mumby, S. M., G. J. Raugi, and P. Bornstein. 1984. Interactions of thrombospondin with extracellular matrix proteins: selective binding to type V collagen. *J. Cell Biol.* 98:646–652.

O'Shea, K. S. 1987. Differential deposition of basement membrane components during formation of the caudal neural tube in the mouse embryo. *Development (Camb.).* 99:509–519.

Patterson, P. H. 1985. On the role of proteases, their inhibitors and the extracellular matrix in promoting neurite outgrowth. *J. Physiol. (Paris).* 80:207–211.

Raugi, G. J., S. M. Mumby, D. Abbott-Brown, and P. Bornstein. 1982. Thrombospondin: synthesis and secretion by cells in culture. *J. Cell Biol.* 95:351–354.

Roberts, D. D., J. A. Sherwood, S. L. Spitalnik, L. J. Panton, R. J. Howard,

Figure 7. Saggital sections through day-17 embryos illustrating TSP deposition in various organs (*a*, *c*, *e*, and *g*), and corresponding phase-contrast micrographs (*b*, *d*, *f*, and *h*). (*a* and *b*) Section through the cerebral cortex illustrating the deposition of TSP on the surface of neuroepithelial cells and in the forming pia (*arrow*). *L*, lumen of neural tube. (*c* and *d*) TSP was deposited in basement membranes of the developing bronchial tree and in the endothelium of the numerous veins (*v*) and arteries in the lung. (*e* and *f*) Forming myotubes illustrate a reduction in cell surface associated TSP (*arrow*) with differentiation. (*g* and *h*) Skin and forming hair follicles, illustrating TSP deposition in the epithelium and at the dermal epidermal junction (*arrow*) and in the basement membrane and epithelium of developing hair follicles (*F*). Bars, 50 μm.

V. M. Dixit, W. A. Frazier, L. H. Miller, and V. Ginsburg. 1985. Thrombospondin binds falciparum malaria parasitized erythrocytes and may mediate cytoadherence. *Nature (Lond.).* 318:64–66.

Roberts, D. D., J. A. Sherwood, and V. Ginsburg. 1987. Platelet thrombospondin mediates attachment and spreading of human melanoma cells. *J. Cell Biol.* 104:131–139.

Rogers, S. L., K. J. Edson, P. C. Letourneau, and S. C. McLoon. 1986. Distribution of laminin in the developing peripheral nervous system of the chick. *Dev. Biol.* 113:429–435.

Sato, Y., K. Mukai, S. Watanabe, M. Goto, and Y. Shimosato. 1986. The AMeX method. A simplified technique of tissue processing and paraffin embedding with improved preservation of antigens for immunostaining. *Am. J. Pathol.* 125:431–435.

Silverstein, R. L., L. L. K. Leung, P. C. Harpel, and R. L. Nachman. 1984. Complex formation of platelet thrombospondin and plasminogen. *J. Clin. Invest.* 74:1625–1633.

Silverstein, R. L., R. L. Nachman, L. L. K. Leung, and P. C. Harpel. 1985. Activation of immobilized plasminogen by tissue activator. *J. Biol. Chem.* 260:10346–10352.

Silverstein, R. L., P. C. Harpel, and R. L. Nachman. 1986. Tissue plasminogen activator and urokinase enhance the binding of plasminogen to TSP. *J. Biol. Chem.* 261:9959–9965.

Sternberg, J., and S. J. Kimber. 1986. Distribution of fibronectin, laminin and entactin in the environment of migrating neural crest cells in early mouse embryos. *J. Embryol. Exp. Morphol.* 91:267–282.

Taraboldi, G., D. D. Roberts, and L. A. Liotta. 1987. Thrombospondin-induced tumor cell migration: haptotaxis and chemotaxis are mediated by different molecular domains. *J. Cell Biol.* 105:2409–2416.

Thiery, J.-P., J.-L. Duband, U. Rutishauser, and G. M. Edelman. 1982. Cell adhesion molecules in early chicken embryogenesis. *Proc. Natl. Acad. Sci. USA.* 79:6737–6741.

Tucker, G. C., M. Delarue, S. Zada, J.-C. Boucaut, and J. P. Thiery. 1988. Expression of the HNK-1/NC-1 epitope in early vertebrate neurogenesis. *Cell Tissue Res.* 251:457–465.

Tuckett, F., and G. M. Morriss-Kay. 1986. The distribution of fibronectin, laminin and entactin in the neurulating rat embryo studied by indirect immunofluorescence. *J. Embryol. Exp. Morphol.* 94:95–112.

Varani, J., V. M. Dixit, S. E. G. Fligiel, P. E. McKeever, and T. E. Carey. 1986. Thrombospondin-induced attachment and spreading of human squamous carcinoma cells. *Exp. Cell Res.* 167:376–390.

Wight, T. M., G. J. Raugi, S. M. Mumby, and P. Bornstein. 1985. Light microscopic immunolocalization of thrombospondin in human tissues. *J. Histochem. Cytochem.* 33:295–302.

Wikner, N., V. M. Dixit, W. A. Frazier, and R. A. F. Clark. 1987. Human keratinocytes synthesize and secrete the extracellular matrix protein thrombospondin. *J. Invest. Dermatol.* 88:207–211.